Ca^{2+} Buffering and Action Potential-Evoked Ca^{2+} Signaling in Dendrites of Pyramidal Neurons

Fritjof Helmchen,* Keiji Imoto,‡ and Bert Sakmann*
*Abteilung Zellphysiologie, Max-Planck-Institut für medizinische Forschung, D-69120 Heidelberg, Germany; and ‡Department of Information Physiology, National Institute for Physiological Sciences, Okazaki 444, Japan

ABSTRACT The effect of the fluorescent Ca^{2+} indicator dye Fura-2 on Ca^{2+} dynamics was studied in proximal apical dendrites of neocortical layer V and hippocampal CA1 pyramidal neurons in rat brain slices using somatic whole-cell recording and a charge-coupled device camera. A single action potential evoked a transient increase of intradendritic calcium concentration ($[Ca^{2+}]_i$) that was reduced in size and prolonged when the Fura-2 concentration was increased from 20 to 250 μM. Extrapolation to zero Fura-2 concentration suggests that "physiological" transients at 37°C have large amplitudes (150–300 nM) and fast decays (time constant <100 ms). Assuming a homogeneous compartment model for the dendrite, 0.5–1% of the total Ca^{2+} entering during an action potential was estimated to remain free. Washout of cytoplasmic Ca^{2+} buffers was not detectable, suggesting that they are relatively immobile. During trains of action potentials, $[Ca^{2+}]_i$ increased and rapidly reached a steady state (time constant <200 ms), fluctuating around a plateau level which depended linearly on the action potential frequency. Thus, the mean dendritic $[Ca^{2+}]_i$ encodes the action potential frequency during physiological patterns of electrical activity and may regulate Ca^{2+}-dependent dendritic functions in an activity-dependent way.

INTRODUCTION

The distribution of Ca^{2+} within dendrites of neurons in the central nervous system is of special interest, because the dendritic trees receive most of the synaptic input and Ca^{2+} is known to regulate neuronal excitability (see Kennedy, 1989) and plasticity (see Bliss and Collingridge, 1993). The dendritic membrane of pyramidal neurons contains voltage-dependent Ca^{2+} channels (Westenbroek et al., 1990; Mills et al., 1994; Magee and Johnston, 1995) and Ca^{2+}-permeable receptor-operated channels, e.g., glutamate receptor channels (Bekkers and Stevens, 1989; Spruston et al., 1995a). In addition, Ca^{2+} may enter dendritic cytoplasm by release from intracellular stores (Alford et al., 1993; Llano et al., 1994). The dynamics of $[Ca^{2+}]_i$ not only depends on the spatiotemporal pattern of Ca^{2+} inflow, but also on localization, mobility, affinity, and kinetics of intradendritic Ca^{2+}-binding molecules, including Ca^{2+} buffering proteins and Ca^{2+} transporters which extrude Ca^{2+} from the cytoplasm (Sala and Hernández-Cruz, 1990; Nowycky and Pinter, 1993; Baimbridge et al., 1992; Clapham, 1995).

Measurements of dendritic Ca^{2+} dynamics in pyramidal neurons using fluorescent indicators have revealed changes in $[Ca^{2+}]_i$ caused by activation of both voltage-dependent Ca^{2+} channels and *N*-methyl-D-aspartate (NMDA)-type glutamate receptor channels (see Regehr and Tank, 1994). Recent experiments demonstrated that subthreshold synaptic activation evokes localized $[Ca^{2+}]_i$ transients in dendritic spines (Yuste and Denk, 1995). In contrast, single action potentials, initiated near the soma, back-propagate actively into apical dendrites of pyramidal neurons (see Stuart and Spruston, 1995) and lead to a global increase of $[Ca^{2+}]_i$ in dendrites (Spruston et al., 1995b; Schiller et al., 1995) and spines (Yuste and Denk, 1995). During a train, action potentials may fail to invade some dendritic branches, restricting the Ca^{2+} signal to parts of the dendritic tree (Jaffe et al., 1992; Spruston et al., 1995b). The functional role and interplay of these different types of dendritic Ca^{2+} signals remain to be elicited.

Ca^{2+} indicators act as additional buffers which compete with endogenous buffers and thereby may significantly alter Ca^{2+} dynamics (Neher and Augustine, 1992; Regehr and Tank, 1994). The effectiveness of a buffer is described by the Ca^{2+}-binding ratio, the ratio of buffer-bound Ca^{2+} changes over free Ca^{2+} changes (see Neher, 1995). Therefore, the interpretation of fluorescence signals depends on the relative Ca^{2+}-binding ratios of endogenous buffers and the exogenous indicator dye. At relatively low dye concentration the fluorescence time course reports the unaltered dynamics of free Ca^{2+}, while at high concentration the dye captures virtually all Ca^{2+} that enters the cytoplasm, resulting in a fluorescence change proportional to the integral Ca^{2+} flux. Dye overload of the cytoplasm therefore has been used to determine fractional Ca^{2+} currents through receptor-coupled ion channels (see Neher, 1995). Measuring undistorted Ca^{2+} dynamics with a low dye concentration, however, is limited by the need for sufficient fluorescence intensity, particularly in small structures like dendrites. Therefore, dendritic $[Ca^{2+}]_i$ measurements using the high-affinity dye Fura-2 in the past were made using unknown or relatively high concentrations (>200 μM). The exact influence of Fura-2 on the measured signals was not known, because no estimate of dendritic Ca^{2+}-binding ratio was available. In other preparations such as striated muscle

Received for publication 29 September 1995 and in final form 1 November 1995.

Address reprint requests to Dr. Bert Sakmann, Abteilung Zellphysiologie, Max-Planck-Institut für medizinische Forschung, Jahnstr. 29, D-69120 Heidelberg, Germany. Tel.: 49-6221-486461; Fax: 49-6221-486459.

0006-3495/96/02/1069/13 $2.00

fibers (Timmerman and Ashley, 1986), *Aplysia* sensory neurons (Blumenfeld et al., 1992) and adrenal chromaffin cells (Neher and Augustine, 1992), Fura-2 was shown to affect Ca^{2+} signals even at low concentration (50 μM). In addition, theoretical studies have shown effects of Fura-2 not only because of its buffering but also its diffusional properties (Sala and Hernández-Cruz, 1990; Nowycky and Pinter, 1993; Wagner and Keizer, 1994).

Here we quantitatively study the effect of the Fura-2 concentration on the size and time course of $[Ca^{2+}]_i$ transients, evoked by single action potentials, in proximal dendrites of neocortical layer V and hippocampal CA1 pyramidal neurons. Endogenous dendritic Ca^{2+}-binding ratios are estimated, assuming a single compartment model for the dendrite. We further investigate dendritic Ca^{2+} accumulation during trains of action potentials using low Fura-2 concentrations, and demonstrate that mean dendritic $[Ca^{2+}]_i$ levels encode the frequency of action potentials during neuronal activity.

MATERIALS AND METHODS

Brain slice preparation and electrophysiology

Brain slices from 12- to 14-day-old Wistar rats were prepared as described previously (Stuart et al., 1993). Briefly, rats were decapitated and 300 μm thick parasagittal neocortical or transversal hippocampal slices were cut in ice-cold solution using a vibratome (Campden Instruments, Loughborough, England). Slices were incubated at 37°C for 45 min and thereafter maintained at room temperature (23–25°C). The solution used for slicing and for perfusion contained (in mM): 125 NaCl, 25 $NaHCO_3$, 25 glucose, 2.5 KCl, 1.25 NaH_2PO_4, 2 $CaCl_2$, and 1 $MgCl_2$, pH 7.4 when bubbled with carbogen (95% O_2, 5% CO_2) (Biometra, Göttingen, Germany). Slices were mounted on an upright epifluorescence microscope (Axioskop FS, Zeiss, Oberkochen, Germany), equipped with a 63× water-immersion objective (numerical aperture 0.9, Achroplan, Zeiss, Germany). Neurons were visually identified using infrared differential interference contrast (IR-DIC) video microscopy (Stuart et al., 1993).

Somatic whole-cell voltage recordings were made with 1.8–4 MΩ patch pipettes using an EPC-7 amplifier (List, Darmstadt, Germany). The pipette solution contained (in mM): 115 potassium gluconate, 20 KCl, 4 Mg-ATP, 10 phosphocreatine, 0.3 GTP, 10 Hepes (pH 7.2, adjusted with KOH), and 20–250 μM Fura-2 (Molecular Probes, Portland, OR). Neurons typically had resting membrane potential levels between −55 and −60 mV. Action potentials were evoked by brief (5–30 ms) depolarizing somatic current injections (110–350 pA in CA1, 350–800 pA in layer V neurons). In some experiments, the patch pipette was retracted after a short whole-cell episode. In these experiments, action potentials were evoked by stimulation with a bipolar electrode placed in layer I (100 μs, 4–30 V). The stimulus threshold for evoking a single action potential was determined before break-in. Voltage recordings were filtered at 3 kHz (eight-pole Bessel filter, Frequency Devices, Haverhill, MA) and digitized at 10 kHz. Stimulation pulses and data acquisition were controlled using a VMEbus computer system (Motorola Delta series 1147, Tampa, FL). All measurements were done at 36–37°C.

Measurement of fast dendritic $[Ca^{2+}]_i$ transients

Fura-2 fluorescence was measured using a 12-bit cooled charge-coupled device (CCD) camera (2 MHz readout rate, TH7883FT chip, ATC-5, Photometrics, Tucson, AZ). To optimize the speed of readout, exposure routines were rewritten in FORTH using lowest level routines and downloaded to the EEPROM of the camera electronics unit. A polychromatic illumination system (bandwidth 12 nm, T.I.L.L. Photonics, München, Germany) allowed determination of the Ca^{2+}-insensitive (isosbestic) excitation wavelength for Fura-2 (356 nm in our system) and fast switching between wavelengths (<3 ms). Excitation light was coupled to the microscope via a light-guide and attenuated with a neutral density filter (optical density 0.1–0.4) to avoid phototoxicity and excessive bleaching. Excitation wavelengths of 356 nm and 380 nm, a 400 nm dichroic mirror and a 410 nm long-pass emission filter were used. Fluorescence data acquisition was controlled using a VMEbus computer system (VDIPS-500, TVIPS, München, Germany) and was synchronized with membrane voltage recordings using a pulse signal from the CCD camera controller.

For high time resolution measurements (100 Hz acquisition rate) the fluorescence signal within a selected rectangular region was binned on-chip in the parallel direction and averaged offline in the serial direction (Schiller et al., 1995). Each 10 ms frame interval included 1 ms of shifting charges beneath the masked CCD area. The contribution of fluorescence from regions outside the selected region to the signal was calculated to be <5%. Autofluorescence from brain slice tissue substantially contributes to background fluorescence with ultraviolet excitation and may change during the experiment (Eilers et al., 1995). Therefore, background fluorescence was measured routinely from a second rectangular region containing no obvious cellular structures. Fluorescence signals were either averaged (10 traces) or digitally filtered with a 3-point binomial filter.

Pyramidal neurons were loaded with Fura-2 via somatic patch pipettes (Fig. 1). A region in the proximal part of the apical dendrite (typically 7 μm wide and 18 μm long, 30–50 μm from the soma) and a background region were selected (Fig. 1 *B*). The dendritic $[Ca^{2+}]_i$ transient, evoked by a single action potential, was used as standard Ca^{2+} signal to study the effect of the concentration of Fura-2. It was measured at 100 Hz with the following protocol (Fig. 1 *D*). Background fluorescence (B_{380} and B_{356}) and isosbestic fluorescence (F_{356}) were measured directly before and after each measurement of fluorescence at 380 nm excitation (F_{380}). A single action potential evoked a transient decrease of F_{380}. The maximal decrease was reached within 1 or 2 sample points, depending on the exact time of occurrence of the action potential. F_{380} did not change, or changed very little, if the current pulse failed to initiate an action potential, indicating that the $[Ca^{2+}]_i$ transient mainly depended on the activation of high voltage-activated Ca^{2+} channels. B_{380}, B_{356}, and F_{356} were interpolated linearly, and the ratio $R = (F_{356} - B_{356})/(F_{380} - B_{380})$ was converted to $[Ca^{2+}]_i$ using the standard ratioing equation (Grynkiewicz et al., 1985). Exponential curves were fitted to the decays of the $[Ca^{2+}]_i$ transients (range 1–2 s, beginning at first point following the peak). The exponential curve was constrained to reach the resting $[Ca^{2+}]_i$ level, which was determined from 20 sample points preceding the action potential, at late time points. The peak amplitude of the $[Ca^{2+}]_i$ transient was defined as the value of the fitted curve above resting level at the first sample point of increase of $[Ca^{2+}]_i$.

Calibration parameters R_{min} and R_{max} (ratios at zero $[Ca^{2+}]_i$ and at $[Ca^{2+}]_i$ levels saturating Fura-2, respectively) were determined by loading neurons with the intracellular solution containing 20 mM EGTA and 20–50 mM $CaCl_2$, respectively. The effective binding constant K_{eff} was determined using the intracellular solution containing 13.3 mM CaEGTA and 6.7 mM EGTA, which was prepared from a Ca^{2+} calibration concentrate kit (Molecular Probes). Fluorescence ratios were measured in a somatic region near the tip of the pipette with low access resistance (≤7 MΩ; Eilers et al., 1995). The dissociation constant (K_d) of Fura-2 for Ca^{2+} binding was 286 nM, calculated from the equation $K_{eff} = K_d(R_{max}/R_{min})$ (Neher and Augustine, 1992) and assuming a dissociation constant of EGTA of 119 nM (pH 7.2, temperature 37°C, and ionic strength 0.15 M; Groden et al., 1991).

Ca^{2+}-binding ratio

The differential Ca^{2+}-binding ratio of a Ca^{2+} buffer X (previously termed Ca^{2+}-binding capacity; see Neher, 1995) is defined as $\kappa_x = \partial[XCa]/\partial[Ca^{2+}]_i$. Because changes in $[Ca^{2+}]_i$ were substantial in our experiments, we used the incremental Ca^{2+}-binding ratio κ'_X (Neher and Augustine, 1992), which

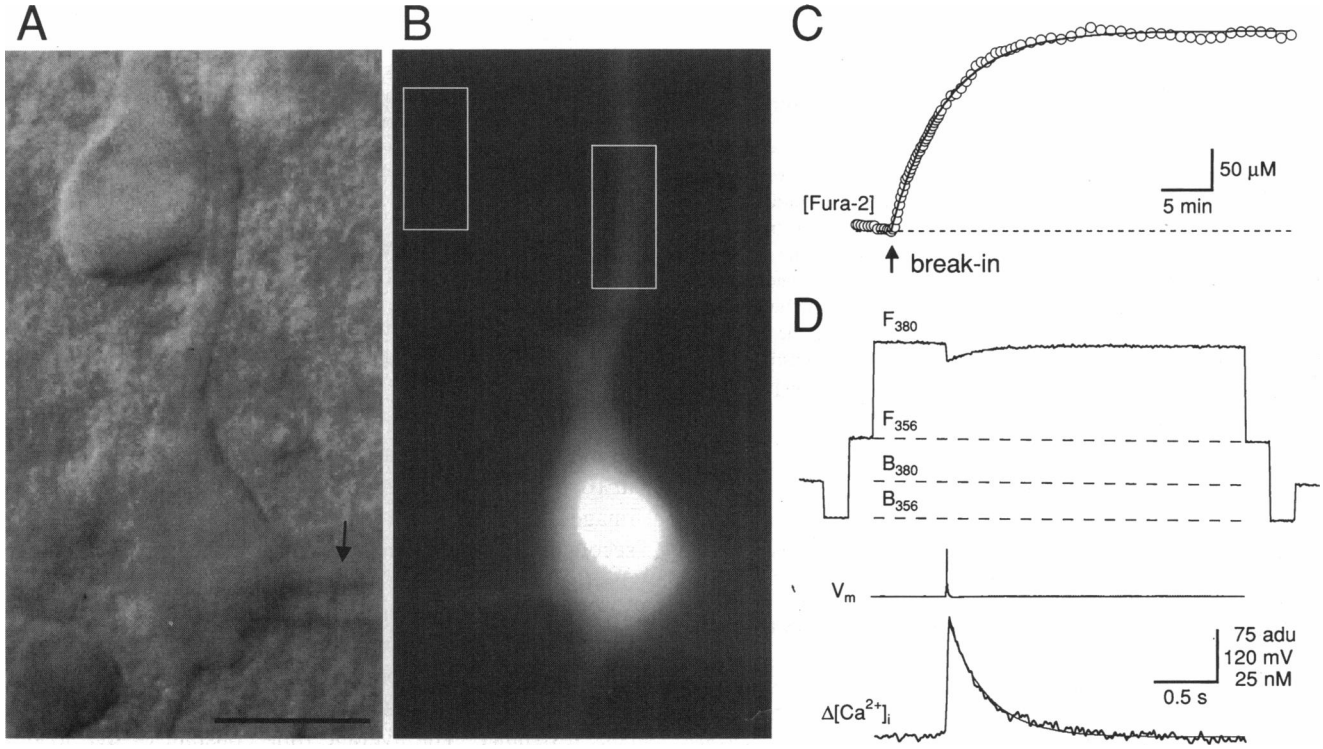

FIGURE 1 Fura-2 measurements in the proximal apical dendrite of pyramidal neurons. (*A*) IR-DIC video image of a layer V pyramidal neuron from rat neocortex with a somatic patch pipette (*arrow*). Scale bar 20 μm. (*B*) Fura-2 fluorescence image taken after 40 min of whole-cell recording (250 μM Fura-2, 356 nm excitation, 300 ms exposure). (*C*) Time course of Fura-2 loading in the proximal dendrite of the neuron shown in *A* and *B*. A series of images was taken during loading, starting in cell-attached configuration (10–60 s intervals, 356 nm excitation, 300 ms exposure). The average fluorescence intensity in a dendritic region (right rectangle in *B*) is shown versus time. Background fluorescence was subtracted (left rectangle in *B*). Fluorescence was converted to Fura-2 concentration assuming full equilibration after reaching the plateau. An exponential curve (*solid line*, time constant 324 s) was fitted to the data. Access resistance increased from 8 to 17 MΩ in this experiment. (*D*) Dendritic $[Ca^{2+}]_i$ transient, evoked by a single action potential, in a different neuron, loaded with 125 μM Fura-2. (*Upper trace*) Raw fluorescence data from a dendritic and a background region (100 Hz acquisition rate, excitation at 356 and 380 nm). Background fluorescence (B_{356}, B_{380}) and dendritic isosbestic fluorescence (F_{356}) values were interpolated linearly (*broken lines*). An action potential (voltage trace V_m) was initiated by a brief somatic current pulse and evoked a decrease of fluorescence at 380 nm excitation (F_{380}). "adu" refers to analog-to-digital units of the CCD camera. (*Lower trace*) Change in $[Ca^{2+}]_i$ from resting level ($\Delta[Ca^{2+}]_i$) after ratiometric conversion of the fluorescence data using the interpolated values of B_{356}, B_{380}, and F_{356}. An exponential curve (*thin line*, time constant 306 ms) was fitted to the decay of the transient. Resting $[Ca^{2+}]_i$ level was 39 nM.

is the ratio of the changes in buffer-bound Ca^{2+} over free Ca^{2+} changes after Ca^{2+} inflow

$$\kappa'_x = \frac{\Delta[XCa]}{\Delta[Ca^{2+}]_i} = \frac{[X]_T K_{d,X}}{([Ca^{2+}]_{rest} + K_{d,X})([Ca^{2+}]_{peak} + K_{d,X})} \quad (1)$$

$[Ca^{2+}]_{rest}$ and $[Ca^{2+}]_{peak}$ are the calcium levels at rest and directly after Ca^{2+} inflow, $[X]_T$ is the total concentration of the buffer, and $K_{d,X}$ is the dissociation constant for Ca^{2+} binding to the buffer X.

Single compartment model of the proximal dendrite

Action potential-evoked dendritic $[Ca^{2+}]_i$ transients can be described by a single compartment model similar to the model used for depolarization-induced $[Ca^{2+}]_i$ transients in chromaffin cells (Neher and Augustine, 1992). Consider a dendritic segment with volume V. An action potential occurring at time t_{AP} causes Ca^{2+} inflow j_{in} through high voltage-activated Ca^{2+} channels. Ca^{2+} inflow is modeled as a δ function $\delta(t - t_{AP})$, increasing the total calcium concentration instantaneously by $\Delta[Ca^{2+}]_T$. Calcium ions are assumed to be partitioned fast within the cytoplasm between an endogenous Ca^{2+} buffer S and the exogenous Ca^{2+} indicator B with constant Ca^{2+}-binding ratios κ_S and κ_B, respectively. Ca^{2+} removal (j_{out}) is modeled as a linear extrusion mechanism with rate constant γ. The resulting differential equation for $[Ca^{2+}]_i$

$$\frac{d[Ca^{2+}]_i}{dt} + \frac{d[SCa]}{dt} + \frac{d[BCa]}{dt} = \frac{(j_{in} - j_{out})}{V}$$

$$\frac{d[Ca^{2+}]_i}{dt}(1 + \kappa_S + \kappa_B) = \Delta[Ca^{2+}]_T \, \delta(t - t_{AP}) \quad (2)$$

$$- \gamma([Ca^{2+}]_i - [Ca^{2+}]_{rest})$$

is solved by an exponential function with amplitude A and decay time constant τ for the change of $[Ca^{2+}]_i$ from resting level:

$$\Delta[Ca^{2+}]_i(t) = [Ca^{2+}]_i - [Ca^{2+}]_{rest}$$

$$= \begin{cases} A \cdot e^{-t/\tau} & t \geq t_{AP} \\ 0 & t < t_{AP} \end{cases} \quad (3)$$

with

$$\tau = \frac{1 + \kappa_S + \kappa_B}{\gamma} \quad \text{and} \quad A = \frac{\Delta[Ca^{2+}]_T}{1 + \kappa_S + \kappa_B} \tag{4}$$

In contrast to Neher and Augustine (1992), no correction for exchange of free and bound Ca^{2+} between the cytoplasm and the pipette solution was made, because the time course of exchange is 4 orders of magnitude slower than the Ca^{2+} extrusion. As seen from Eq. 4, the $[Ca^{2+}]_i$ transient is reduced in amplitude and its decay is slowed by increasing the amount of exogenous Ca^{2+}-binding ratio κ_B. Because of the linear dependence of τ and A^{-1}, the inverse of the amplitude, on κ_B, an experimental estimate of the endogenous Ca^{2+}-binding ratio κ_S can be obtained from the negative x axis intercept of a plot of τ or A^{-1} versus κ_B (Neher and Augustine, 1992). The time integral of the transient, given by the product $A\tau$ of amplitude and time constant, however, is independent of κ_B:

$$\int_{t_{AP}}^{\infty} \Delta[Ca^{2+}]_i\,(t)\,dt = A\tau = \frac{\Delta[Ca^{2+}]_T}{\gamma} \tag{5}$$

A second method to estimate the endogenous Ca^{2+}-binding ratio κ_S is based on the analysis of the amount of Ca^{2+} bound to Fura-2. Assuming the integral of the Ca^{2+} current during an action potential to be a constant, it follows from Eq. 24 of Neher and Augustine (1992)

$$\Delta F_{380} = \Delta F_{max}\,\kappa_B/(1 + \kappa_B + \kappa_S) \tag{6}$$

where ΔF_{380} is the change in fluorescence intensity with excitation at 380 nm, and ΔF_{max} is the maximal fluorescence change, which ΔF_{380} approaches when the cell is overloaded with Fura-2 and all entering calcium ions are taken up by Fura-2 ($\kappa_B \gg \kappa_S$).

Summation of $[Ca^{2+}]_i$ transients

During a train of action potentials dendritic $[Ca^{2+}]_i$ transients sum. We assume linear superposition of transients with amplitude A and time constant τ and consider a train of action potentials with interval Δt between action potentials (constant action potential frequency $\nu_{AP} = 1/\Delta t$) beginning at $t = 0$ (see also Regehr et al., 1994). The $[Ca^{2+}]_i$ level above resting immediately before the (n+1)-th action potential is given by a geometric progression:

$$\Delta[Ca^{2+}]\,(n\Delta t) = A\sum_{i=1}^{n} e^{-(i\Delta t)/\tau} = A\left(\sum_{i=0}^{n}(e^{-\Delta t/\tau})^i - 1\right)$$

$$= \frac{A}{(e^{\Delta t/\tau} - 1)}\,(1 - e^{-(n\Delta t)/\tau}) \tag{7}$$

This determines the time course of the lower envelope of the signal. Thus, $[Ca^{2+}]_i$ exponentially reaches a steady state and then fluctuates between a lower and an upper level. The time to reach steady state is determined by the time constant τ independent of the stimulation frequency ν_{AP}. The steady state is reached when the decay of $[Ca^{2+}]_i$ during an interval Δt is just compensated by the increase A evoked by the next action potential. The lower and upper steady state $[Ca^{2+}]_i$ levels P_l and P_u are calculated from Eq. 7 as $n \to \infty$:

$$P_l = \frac{A}{(e^{\Delta t/\tau} - 1)} \quad \text{and} \quad P_u = P_l + A = \frac{A}{(1 - e^{-\Delta t/\tau})} \tag{8}$$

After reaching steady state, the mean $[Ca^{2+}]_i$ level above resting $[Ca^{2+}]_i$ ($<\Delta[Ca^{2+}]_i>$) is given by the time integral of $[Ca^{2+}]_i$ during one stimulus interval:

$$<\Delta[Ca^{2+}]_i> = \frac{1}{\Delta t}\int_0^{\Delta t} P_u e^{-t/\tau} dt = \frac{A\tau}{\Delta t} = A\tau\,\nu_{AP} \tag{9}$$

This is a simple relationship between the mean dendritic $[Ca^{2+}]_i$ level and the frequency of action potentials generated by the neuron. A rise to mean $[Ca^{2+}]_i$ levels above the single response amplitude A occurs if $\nu_{AP} > 1/\tau$. At the end of a train of action potentials, $[Ca^{2+}]_i$ exponentially decays back to resting level with time constant τ.

RESULTS

Time course of Fura-2 loading of the proximal apical dendrite

Neocortical layer V neurons with an apical dendrite parallel to the surface of the brain slice were selected using IR-DIC video microscopy (Fig. 1 *A*), and the time course of Fura-2 loading via a somatic patch pipette was measured. After forming a Gigaohm seal, acquisition of fluorescence images in 10–60 s intervals began. After break-in, the fluorescence image of the proximal part of the neuron appeared within seconds and the fluorescence intensity increased until it reached a stable value (Fig. 1 *B*). The time course of the average fluorescence intensity within a dendritic region is shown in Fig. 1 *C*. Exponential curves were fitted to the data, although data points sometimes deviated from an exponential rise, probably due to an increasing pipette access resistance. The average time constant of dye loading was 203 ± 21 s in proximal dendritic regions (n = 13, mean ± SEM). For comparison, somatic regions (not containing the nucleus) of the same neurons were analyzed and revealed an only slightly faster loading time constant of 181 ± 21 s. Initial access resistance varied between 6 and 9 MΩ and increased to 10–18 MΩ after 20 min of whole-cell recording. The speed of loading clearly depended on access resistance, being faster with lower access resistance. We conclude that 10 min of somatic loading is sufficient to equilibrate the Fura-2 concentration in the cytoplasm of the proximal apical dendrite with the concentration in the pipette solution, provided the access resistance is kept <10 MΩ.

Dendritic $[Ca^{2+}]_i$ transients depend on Fura-2 concentration

Neurons were loaded with different Fura-2 concentrations ranging from 20 to 250 μM. After loading for at least 10 min with an access resistance of <10 MΩ, dendritic $[Ca^{2+}]_i$ transients were evoked by single action potentials and measured at an acquisition rate of 100 Hz (Fig. 1 *D*; see Materials and Methods). $[Ca^{2+}]_i$ transients were larger and decayed faster when measured with lower concentration of Fura-2 (Fig. 2 *A*). The concentration of Fura-2 was converted to Fura-2 Ca^{2+}-binding ratio κ_B' according to Eq. 1. The decay time constant τ, obtained from 94 layer V pyramidal neurons, clearly depended on κ_B', even with the relatively low range of concentration used (Fig. 2 *B*). To estimate the time course of unaltered $[Ca^{2+}]_i$ transients, a regression line to the data was extrapolated to zero Fura-2 Ca^{2+}-binding ratio κ_B' and revealed a time constant of 55 ms. According to Eq. 4, the negative x axis intercept of the

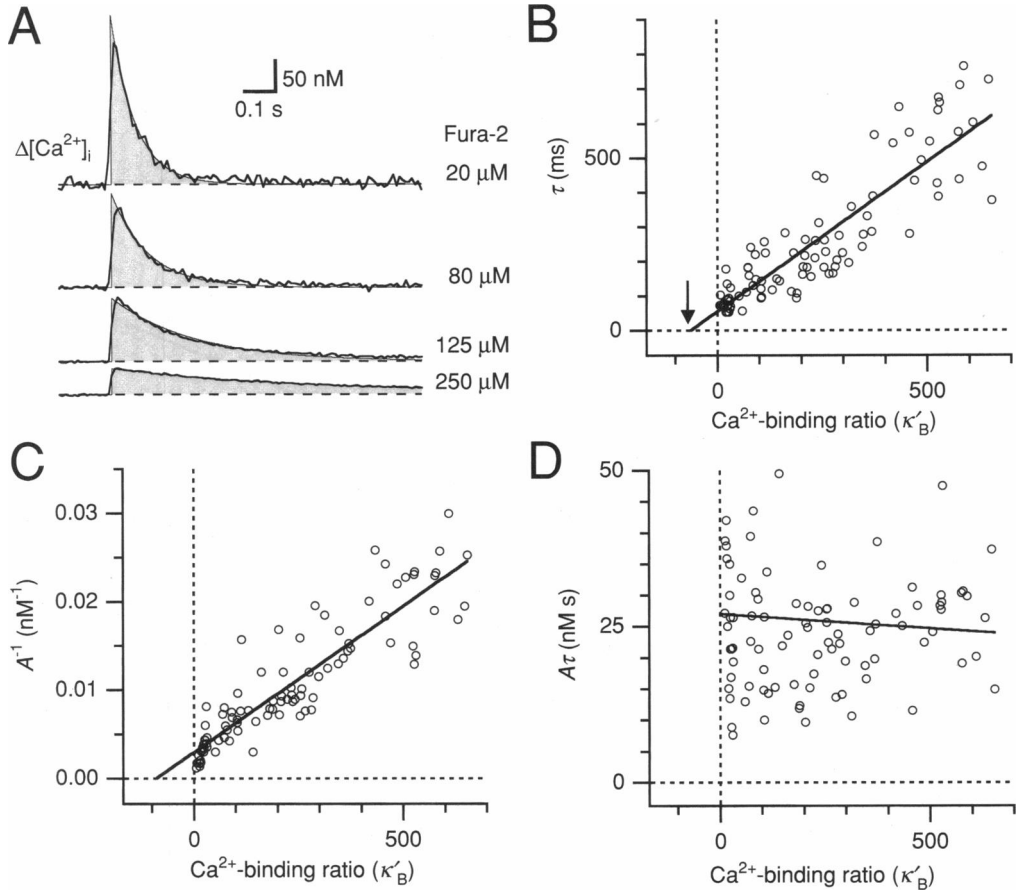

FIGURE 2 Dependence of dendritic $[Ca^{2+}]_i$ transients on Fura-2 Ca^{2+}-binding ratio. (*A*) $[Ca^{2+}]_i$ transients, evoked by single action potentials, measured in the proximal dendrites of four different layer V pyramidal neurons somatically loaded with 20, 80, 125, and 250 μM Fura-2, respectively. Each trace is an average of 10 sweeps. Exponential curves (*thin lines filled to zero*) were fitted to the decays of the transients (time constants of 78, 117, 265, and 703 ms, respectively). Grey areas represent the integral $A\tau$, the product of peak amplitude A, and time constant τ of the fitted curves. (*B*) Decay time constant τ as a function of Fura-2 Ca^{2+}-binding ratio κ_B' (n = 94). Fura-2 concentration range was 20–250 μM. A regression line (*solid line*, regression coefficient r = 0.88) is extrapolated to the negative x axis intercept, which gives an estimate for the endogenous Ca^{2+}-binding ratio κ_S (*arrow*). (*C*) Plot of the inverse of the amplitude A^{-1} as a function of κ_B'. Also shown is a regression line (*solid line*, r = 0.90). (*D*) The integral $A\tau$ versus κ_B'. Linear regression (*solid line*, r = −0.08) revealed no significant dependence of $A\tau$ on κ_B'. Mean resting $[Ca^{2+}]_i$ level was 64 ± 4 nM.

regression line provides κ_S = 63 as an estimate of the endogenous Ca^{2+}-binding ratio. A similar dependence on κ_B' was seen for A^{-1}, the inverse of the amplitude of the $[Ca^{2+}]_i$ transients (Fig. 2 *C*). Extrapolation of a regression line revealed an amplitude of 337 nM at κ_B' = 0 and 90 as an estimate of κ_S. Although there was large scattering, the integral of the $[Ca^{2+}]_i$ transients $A\tau$ did not significantly depend on κ_B' (Fig. 2 *D*). Similar measurements were made on proximal apical dendrites of 53 hippocampal CA1 neurons (not shown). Extrapolated values for amplitude and decay time constant at κ_B' = 0 were 303 nM and 166 ms, respectively. Estimates of the endogenous Ca^{2+}-binding ratio κ_S were 64 and 186, obtained from plots of amplitude and time constant versus κ_B', respectively.

Dendritic Ca^{2+}-binding ratio determined in single neurons

The pooled data from 94 individual neurons (Fig. 2) show a clear dependence of size and time course of dendritic $[Ca^{2+}]_i$ transients on Fura-2 concentration and provide a range of 60–190 as estimate of κ_S. But the data scatter considerably, which could reflect differences in the Ca^{2+}-binding ratio of different cells. To determine the dependence on Fura-2 concentration in single neurons, standard measurements of $[Ca^{2+}]_i$ transients, evoked by single action potentials, were made during Fura-2 loading (Fig. 3 *A*). Regions for fluorescence measurement were selected before break-in based on the IR-DIC video image. Fura-2 concentration was measured using the isosbestic fluorescence intensity $I_{356} = F_{356} - B_{356}$, assuming full loading after the fluorescence reached a plateau level.

Analysis of the amplitude and the decay of the dendritic $[Ca^{2+}]_i$ transients revealed clear changes during loading of layer V dendrites with 125 μM Fura-2. Estimates of amplitude and decay time constant at zero Fura-2 Ca^{2+}-binding ratio κ_B' and of the endogenous Ca^{2+}-binding ratio were obtained by linear regression and extrapolation (Fig. 3 *B*) in 13 layer V neurons. The

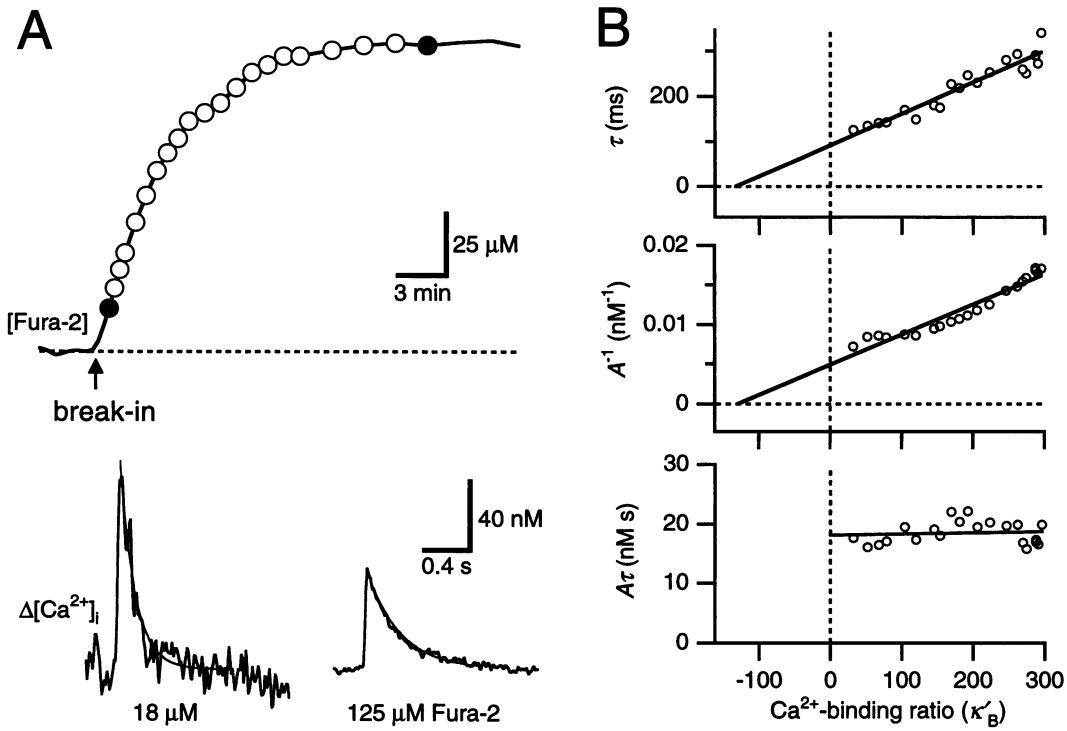

FIGURE 3 Dendritic $[Ca^{2+}]_i$ transients during Fura-2 loading. (*A*) The proximal dendrite of a layer V neuron was loaded with 125 μM Fura-2 (*upper panel*). Standard measurements of dendritic $[Ca^{2+}]_i$ transients (see Fig. 1 *D*) were made during loading every 20–60 s (○). $[Ca^{2+}]_i$ transients measured directly after break-in and after full loading (●) are shown in the lower panel. Exponential curves fitted to their decays had time constants of 126 and 291 ms, respectively (*thin lines*). (*B*) Decay time constant τ, the inverse of the amplitude A^{-1}, and the integral $A\tau$ as a function of Fura-2 Ca^{2+}-binding ratio κ'_B. Linear regressions revealed a time constant of $\tau = 92$ ms and an amplitude of $A = 203$ nM at $\kappa'_B = 0$ in this experiment ($r = 0.96$ for both). Negative x axis intercepts were 132 and 129, respectively.

results agree well with those obtained from the pooled data, but the scatter was much less ($r = 0.94 \pm 0.01$, $n = 13$). Similar results were obtained from loading 5 CA1 pyramidal neurons with 200 μM Fura-2. Table 1 summarizes the estimates of unaltered size and time course of action potential-evoked $[Ca^{2+}]_i$ transients as well as of the endogenous Ca^{2+}-binding ratio κ_S in layer V and CA1 dendrites, and shows that neocortical and hippocampal pyramidal neurons behave similarly with respect to action potential evoked Ca^{2+} signals in their proximal apical dendrites.

From the Fura-2 loading experiments in single cells it was also possible to estimate the endogenous Ca^{2+}-binding ratio κ_S by analyzing the action potential-evoked fluorescence decrements ΔF_{380} (Fig. 4 *A*). Fluorescence decrements ΔF_{380} as a function of κ'_B could be reasonably described according to Eq. 6, yielding another estimate of κ_S (Fig. 4 *B*). The estimates of κ_S, obtained from analysis of either decay time constant, amplitude, or fluorescence decrement, agree well (Table 1).

Mobility of endogenous Ca^{2+} buffers

Loading neurons with indicator dyes using the whole-cell configuration may cause "washout" of diffusible cytoplasmic components, e.g., mobile Ca^{2+} buffers (Zhou and Neher, 1993). To minimize a possible washout effect, five layer V neurons were loaded during a short period (<30 s) via whole-cell patch pipettes containing a high concentra-

TABLE 1 Ca^{2+} dynamics in proximal apical dendrites of pyramidal neurons

		Single action potential-evoked $[Ca^{2+}]_i$ transient		Endogenous Ca^{2+}-binding ratio κ_S		
	n	Amplitude A (nM)*	Decay time constant τ (ms)*	From A^{-1}	From τ	From ΔF_{380}
Layer V‡	13	262 ± 25	70 ± 7	126 ± 21	105 ± 14	135 ± 17
CA1§	5	151 ± 19	92 ± 25	168 ± 61	187 ± 45	207 ± 56

*Values from extrapolation to zero Fura-2 Ca^{2+}-binding ratio.
‡Loading with 125 μM Fura-2.
§Loading with 200 μM Fura-2.
Values are given as mean ± SEM.

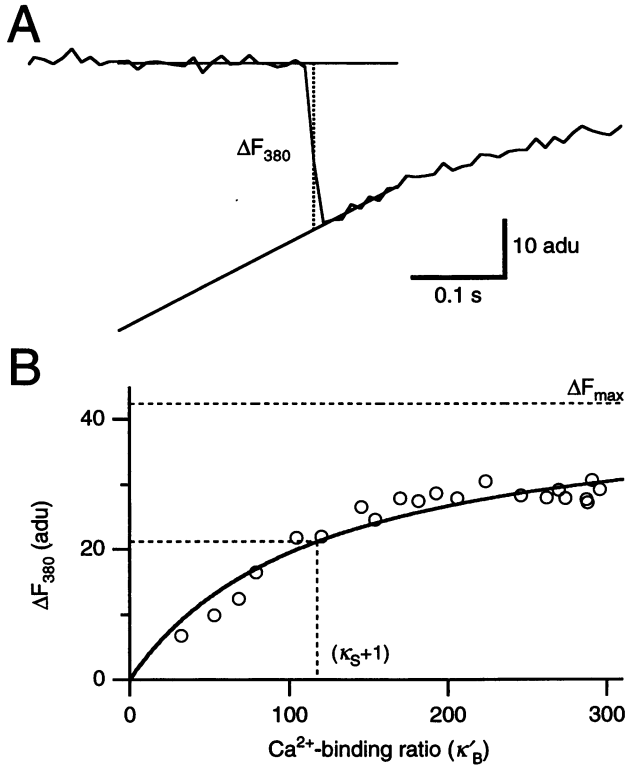

FIGURE 4 Analysis of fluorescence decrements. (*A*) Fluorescence decrement at 380 nm excitation (ΔF_{380}) evoked by a single action potential (125 μM Fura-2). ΔF_{380} was evaluated at the first sample point deviating from baseline. A line was fitted to eight data points after the maximal decrease and back-extrapolated to the first sample point of fluorescence decrease. (*B*) Plot of the fluorescence decrements ΔF_{380}, measured during the Fura-2 loading shown in Fig. 3 *A*, versus Fura-2 Ca^{2+}-binding ratio κ'_B. ΔF_{max} and κ_S were obtained from a fit according to Eq. 6 (*solid line*). The endogenous Ca^{2+}-binding ratio κ_S corresponds to the half-maximal value of ΔF_{380} and was 115 in this experiment.

tion of Fura-2 (2 mM). After break-in, the isosbestic fluorescence intensity I_{356} rapidly increased (Fig. 5 *A*, *upper panel*). After 10–20 s of whole-cell recording the pipette was retracted and an outside-out patch was formed within 30 s. After retraction of the pipette I_{356} decreased again, indicating that the Fura-2 concentration in the proximal part of the neuron now decreased due to diffusional equilibration of Fura-2 within the neuron. The peak of I_{356} in Fig. 5 *A* was estimated to correspond to about 200 μM Fura-2 by recording from the neuron a second time with a pipette containing 125 μM Fura-2 and comparing the fluorescence intensities. However, an exact conversion of Fura-2 concentration to Ca^{2+}-binding ratio was difficult because of an initial fluorescence offset in the dendritic region, probably caused by extracellular Fura-2 or scattered light from the pipette.

With decreasing Fura-2 concentration dendritic $[Ca^{2+}]_i$ transients evoked by single action potentials increased in size and became faster (Fig. 5 *A*, *lower panel*). The time constant τ and the amplitude A depended on I_{356}, with extrapolated values of 99 ± 7 ms and 305 ± 44 nM at $I_{356} = 0$, respectively ($n = 5$; Fig. 5 *B*). The integral $A\tau$ did not change significantly with decreasing I_{356}. The finding that the alteration of $[Ca^{2+}]_i$ transients by Fura-2 was similar after short loading with subsequent equilibration and during continuous loading with 125 μM Fura-2 suggests that there is no significant washout of mobile endogenous Ca^{2+} buffers during the first 10–15 min of whole-cell recording.

Dendritic Ca^{2+} accumulation during trains of action potentials

In vivo pyramidal neurons respond to a sensory stimulus with a train of action potentials (Burne et al., 1984; Simons et al., 1992). Therefore we measured the buildup of dendritic $[Ca^{2+}]_i$ during trains of action potentials. To minimize alteration of the Ca^{2+} signal, low concentrations of Fura-2 (20–50 μM) were used.

Ca^{2+} accumulation in proximal dendrites of layer V neurons was measured during 2 s trains of action potentials with constant frequencies ranging from 2 to 30 Hz. $[Ca^{2+}]_i$ rapidly reached a steady state and then fluctuated around a plateau level that depended on action potential frequency (Fig. 6 *A* and *B*). A line was fitted to the data points of mean $[Ca^{2+}]_i$ plateau level versus action potential frequency (Fig. 6 *B*). The slope of this line agreed well with the proportionality constant $A\tau$ according to Eq. 9, suggesting linear superposition of the $[Ca^{2+}]_i$ transients. The ratio of $A\tau$ to the fitted slope was between 0.82 and 1.37, with an average value of 1.04 ± 0.06 (n = 10). The integral $A\tau$ was calculated from amplitude A and time constant τ, which were obtained from an exponential fit to the $[Ca^{2+}]_i$ transient evoked by a single action potential. The time to reach steady state was quantified by fitting exponential curves to the lower envelope of the Ca^{2+} signals at 10 and 20 Hz stimulation according to Eq. 7 (Fig. 6 *C*). On average, time constants were 162 ± 30 ms and 142 ± 21 ms at 10 and 20 Hz, respectively ($n = 8$). Similar results were obtained in 3 CA1 neurons.

Decay of $[Ca^{2+}]_i$ after trains of action potentials

Assuming linear superposition of monoexponentially decaying $[Ca^{2+}]_i$ transients, $[Ca^{2+}]_i$ decays back to resting level after a train of action potentials with the time constant τ. However, in all our experiments the decay of $[Ca^{2+}]_i$ after a train could not be fitted satisfactory with a monoexponential curve; rather, two exponential components were needed (Fig. 7 *A*). The relative amplitude of the slow component was ~25%, and the fast and slow decay time constant were about 0.1 and 1 s, respectively. To establish whether decay time constants or relative amplitudes depended on the action potential frequency, the sum of two exponential curves was fitted to the decay of $[Ca^{2+}]_i$ after 2 s trains of action potentials with frequencies between 5 and 30 Hz. Decay time constants increased only slightly with action potential frequency (Fig. 7 *B*), whereas the relative

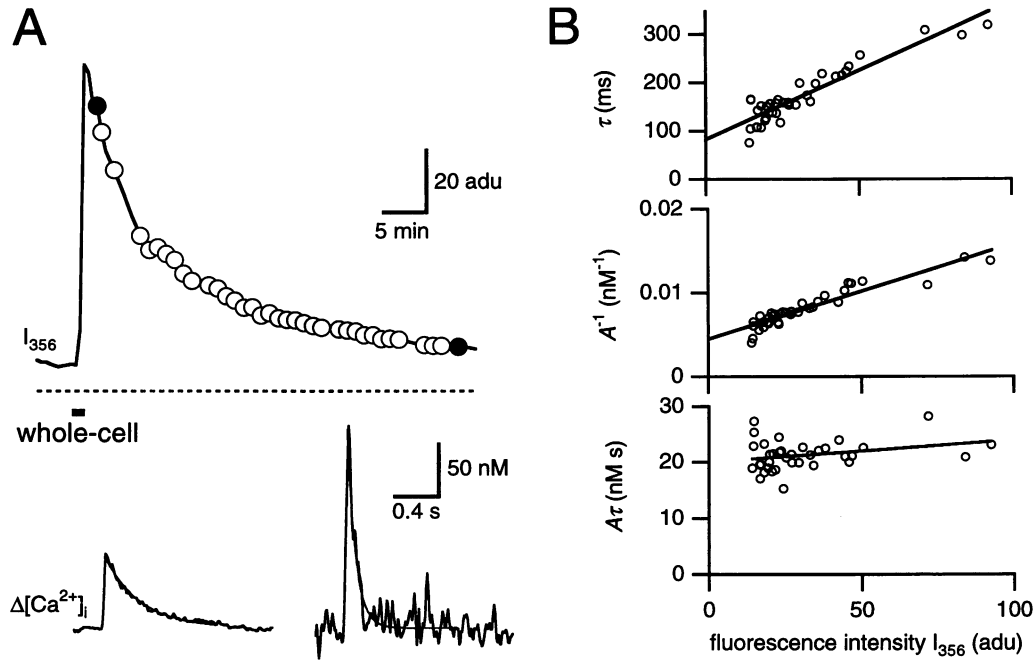

FIGURE 5 Dendritic $[Ca^{2+}]_i$ transients following a short whole-cell recording period. (*A*) Time course of the isosbestic fluorescence intensity I_{356} in analog-to-digital units (adu) after 20 s whole-cell recording with a somatic patch pipette containing 2 mM Fura-2 (*upper panel*). Standard measurements of dendritic $[Ca^{2+}]_i$ transients (see Fig. 1 *D*) were made during equilibration of Fura-2 within the neuron (○). Single action potentials were initiated by synaptic stimulation. The $[Ca^{2+}]_i$ transients measured directly following the short whole-cell recording period and after Fura-2 equilibration (●) are shown in the lower panel. (*B*) Plots of the decay time constant τ, the inverse of the amplitude A^{-1}, and the integral $A\tau$ versus the isosbestic fluorescence intensity I_{356}. Solid lines are regression lines of the data. Extrapolation to $I_{356} = 0$ revealed a time constant of $\tau = 82$ ms and an amplitude of $A = 224$ nM in this experiment ($r = 0.93$ for both).

amplitudes were independent of action potential frequency (Fig. 7 *C*).

Dendritic $[Ca^{2+}]_i$ level encodes the frequency of action potentials

The finding that dendritic $[Ca^{2+}]_i$ transients summate linearly suggests that the mean dendritic $[Ca^{2+}]_i$ level encodes the frequency of action potentials. Even if the frequency is changing, $[Ca^{2+}]_i$ reaches a new steady state rapidly (<0.2 s; Fig. 6 *C*), and thus the mean level may be able to follow changes in action potential frequency during electrical activity. According to Eq. 9, the proportionality constant between $[Ca^{2+}]_i$ level and action potential frequency is given by the integral $A\tau$ (in units of nM/Hz).

To demonstrate encoding of action potential frequency by the dendritic $[Ca^{2+}]_i$ level directly, three layer V pyramidal neurons were loaded with a low concentration of Fura-2 (20 μM), and $[Ca^{2+}]_i$ in the proximal dendrite was measured during simulated "physiological" neuronal activity (Fig. 8). Bursts of action potentials with variable frequency were evoked by varying the amount of somatic current injection (Fig. 8 *A*, *upper trace*). The instantaneous action potential frequency was derived from the action potential pattern by finding for each action potential the time when the voltage crossed a −5 mV threshold (t_i), and defining $1/\Delta t = 1/(t_{i+1} - t_i)$ for $t_i \le t < t_{i+1}$ (Fig. 8 *A*, *middle trace*). The simultaneously measured change in calcium concentration $\Delta[Ca^{2+}]_i$ superimposed well with $1/\Delta t$ in the frequency range up to 30 Hz (Fig. 8 *A*, *lower trace*). If $\Delta[Ca^{2+}]_i$ was divided by $A\tau$ to convert the Ca^{2+} signal to "frequency," even the absolute values agreed well. Sometimes during current injection, however, two action potentials occurred within 5–10 ms. These short high frequency bursts of action potentials led to peaks of 100–200 Hz in the frequency curve $1/\Delta t$, which are truncated in Fig. 8 *A* (*arrows*). Because of their brief duration, they are not resolved in the Ca^{2+} signal. Nevertheless, groups of action potentials with different frequencies in the range up to 30 Hz are well separated in the Ca^{2+} signal (Fig. 8 *B*).

DISCUSSION

Fura-2 measurements in proximal dendrites

Fluorescence measurements were restricted to the initial portion of the proximal apical dendrite because of its relatively large volume and because the Fura-2 concentration could be controlled by loading neurons via low resistance somatic patch pipettes. Although the acquisition rate of cooled CCD cameras is limited by the slow readout rate, restriction to subarrays and on-chip binning allow measurements with relatively high time resolution (Lasser-Ross et

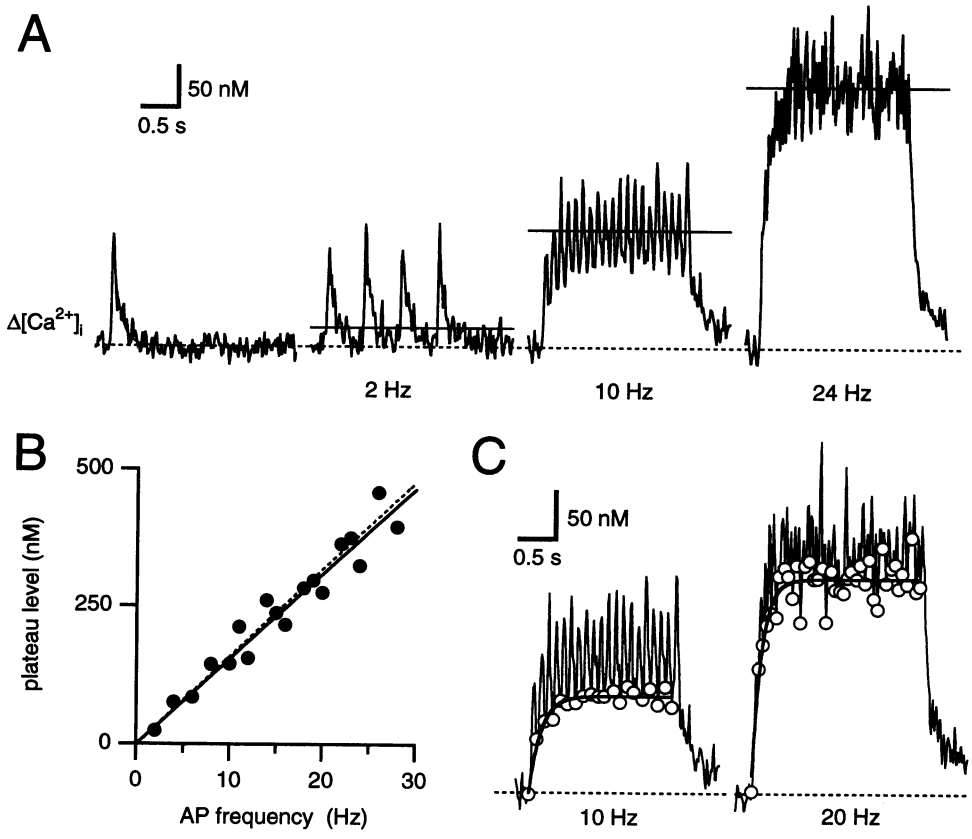

FIGURE 6 Ca^{2+} accumulation during trains of action potentials. (*A*) $[Ca^{2+}]_i$ signals in the proximal apical dendrite of a layer V pyramidal neuron evoked by a single action potential (*left*, exponential fit: A = 146 nM, τ = 103 ms) and during 2 s trains of action potentials at 2, 10, and 24 Hz. Each action potential was evoked by a 10–30 ms somatic current pulse. 50 μM Fura-2 was used to provide a sufficient signal-to-noise ratio without having to average. The mean $[Ca^{2+}]_i$ levels during the last second of stimulation are shown as solid horizontal lines. (*B*) Mean dendritic $[Ca^{2+}]_i$ level above resting $[Ca^{2+}]_i$ during the last second of stimulation plotted versus the frequency of action potentials (AP). Also shown are a fitted line through the origin with slope 15.9 nM/Hz (- - - -) and a line with slope $A\tau$ = 15 nM/Hz according to Eq. 9 (——). (*C*) An exponential rise was fitted to the lower envelope (○) of the $[Ca^{2+}]_i$ signals with 10 and 20 Hz stimulation (time constants of 158 and 111 ms, respectively).

al., 1991; Schiller et al., 1995). The signal-to-noise ratio achieved in such a way was sufficient to resolve fast $[Ca^{2+}]_i$ transients in proximal dendrites of neurons loaded with as little as 20 μM Fura-2, which is about 10 times less than used previously for dendritic $[Ca^{2+}]_i$ measurements. The time constant for loading somata of layer V neurons with Fura-2 with 10 MΩ access resistance (3 min) is ~3 times the value found for chromaffin cells by Pusch and Neher (1988), presumably because of the larger volume of pyramidal cell somata. Diffusional equilibration in distal dendritic processes takes significantly longer and no longer follows an exponential time course (Rexhausen, 1992). However, in the initial portion of apical dendrites the Ca^{2+}-insensitive fluorescence reached a plateau level in a roughly exponential manner, with a time constant only 20 s larger than in the soma. This indicates that the tip of the loading pipette is the major diffusional barrier (Pusch and Neher, 1988) and that Fura-2 equilibrates rapidly within the proximal part of the neuron.

Single compartment model of the dendrite

For quantitative analysis the proximal dendrite was treated as a single, homogeneous compartment, assuming instantaneous Ca^{2+} inflow and rapid diffusional equilibration. How reasonable are these assumptions? Action potentials backpropagate into dendrites of neocortical layer V pyramidal cells with a conduction velocity of >300 μm/ms at 35°C (Stuart and Sakmann, 1994). Therefore, the action potential occurs nearly instantaneously along a 20 μm long dendritic segment and the duration of Ca^{2+} inflow during the repolarizing phase of the action potential is probably <2 ms (McCobb and Beam, 1991; Markram et al., 1995). Thus, the assumption of instantaneous inflow is valid. The time for diffusional equilibration is shorter than our estimate of the decay time constant of the $[Ca^{2+}]_i$ transient (70 ms), but may last a significant portion of it. For a dendritic radius of a = 1–2 μm and a Ca^{2+} diffusion constant of D_{Ca} = 300 $\mu m^2\ s^{-1}$ (Zhou and Neher, 1993), a characteristic time for diffusional equilibration, given by a^2/D_{Ca}, is between 3 and 13 ms. In addition, buffers with a slow on-rate may not have a chance to bind Ca^{2+} according to their equilibrium constant during a 70 ms period. Therefore, it is likely that more complex or nonequilibrium effects have to be considered within dendrites. Nevertheless, assuming that only endogenous buffers that effectively compete with Fura-2 (having a similar on-rate) contribute to the buffer pool S, the homogeneous compartment model for the dendrite is a valuable simplification.

Physiological $[Ca^{2+}]_i$ transients

Ca^{2+} inflow during an action potential into proximal apical dendrites of pyramidal neurons mainly occurs through high voltage-activated Ca^{2+} channels of the L-, N- and P-type (Markram et al., 1995; Christie et al., 1995). Ca^{2+} release

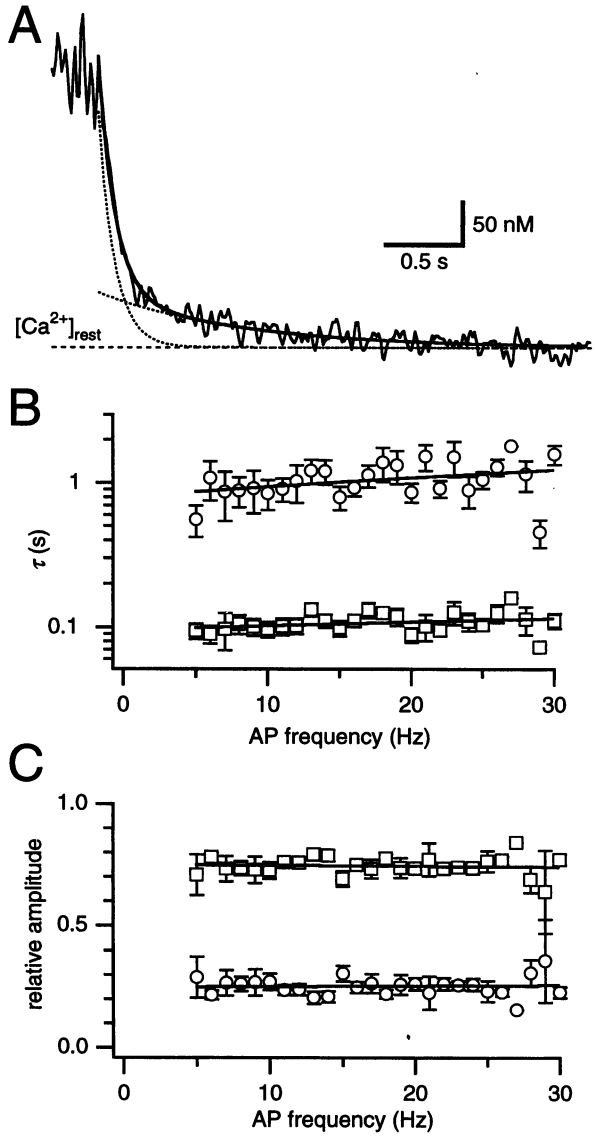

FIGURE 7 $[Ca^{2+}]_i$ decay after a train of action potentials. (*A*) Decay of $[Ca^{2+}]_i$ after a 2 s train of action potentials at 24 Hz (same trace as in Fig. 7 *A*). A double exponential curve was fitted to the decay (——). The fast and slow component (· · · ·) had time constants of 84 and 727 ms, respectively. (*B*) Decay time constant of the fast (□) and the slow (○) component versus action potential frequency (n = 7, mean ± SEM). Solid lines are linear regressions of the data with slopes of 0.6 and 14 ms per Hz, respectively. (*C*) Relative amplitudes of the fast (□) and the slow (○) component versus action potential frequency (n = 7, mean ± SEM). Solid lines are linear regressions (slope = 0.03% per Hz).

from internal stores does not contribute to the evoked $[Ca^{2+}]_i$ transient in layer V pyramidal neurons, and dendritic Ca^{2+} is mostly removed by uptake into the endoplasmic reticulum and extrusion across the plasma membrane via ATP-dependent Ca^{2+} transporters (Markram et al., 1995).

Regehr and Tank (1992) have shown that Fura-2 at 250–600 μM markedly reduces the amplitude and slows the decay of $[Ca^{2+}]_i$ transients in proximal dendrites of CA1 neurons. Here we show a reduction and slowing of action potential-evoked transients by concentrations between 20 and 250 μM. To estimate the undistorted size and time course of the transients we extrapolated the amplitude and decay time constant to zero Fura-2 Ca^{2+}-binding ratio. This is justified because washout of mobile endogenous Ca^{2+} buffers, if present at all, is small during the first 10–15 min of whole-cell recording (see below). Extrapolation revealed an amplitude of 150–300 nM and a decay time constant of 70–90 ms at 37°C for the $[Ca^{2+}]_i$ transient evoked by a single action potential. The transient was reduced and prolonged by a factor of about three with 125 μM Fura-2 (Figs. 2 and 3). Thus, our measurements are consistent with previous measurements using patch pipettes and Fura-2 at 150 μM (Spruston et al., 1995b; Schiller et al., 1995). In addition, our estimate of the decay time constant agrees well with fluorescence decay time constants measured using low concentrations of Calcium-Green 1 or Fluo-3 in layer V dendrites (Markram et al., 1995). Previous measurements using sharp microelectrodes for Fura-2 loading revealed an amplitude of ~5–10 nM and a decay time constant of >600 ms in CA1 dendrites (Jaffe et al., 1992; Miyakawa et al., 1992; Jaffe et al., 1994). Although there may be differences in experimental conditions or calibration, these values are explained by assuming that the concentration of Fura-2 was >300 μM in these experiments.

One may argue that the slowing of $[Ca^{2+}]_i$ transients during Fura-2 loading could result from a decrease of γ, the rate of Ca^{2+} clearance, e.g., by insufficient ATP support to the Ca^{2+}-ATPases, since the time constant depends inversely on γ (Eq. 4). However, this is unlikely because the ATP affinity of Ca^{2+}-ATPases is in the low micromolar range (Carafoli and Chiesi, 1992), and 4 mM ATP was included in the pipette solution. In addition, a changing rate of Ca^{2+} clearance during loading would change the integral $A\tau$ as well (Eq. 5), which was not the case.

Dendritic Ca^{2+} buffers

A first step in characterizing the endogenous buffering of Ca^{2+} is to estimate the ratio of total over free $[Ca^{2+}]$ changes after Ca^{2+} inflow, which is given by $(1 + \kappa_S)$. We found that 0.5–1% of the total Ca^{2+} entering proximal dendrites of layer V and CA1 neurons during an action potential remain free, corresponding to a Ca^{2+}-binding ratio κ_S between 100 and 200 (Table 1). This estimate may be subject to errors, e.g., all three approaches for estimation are based on the Fura-2 Ca^{2+}-binding ratio, which depends inversely on the chosen K_d of Fura-2. However, this is unlikely to result in an uncertainty factor of >1.5. In other cells such as *Aplysia* neurons, melanotrophs of the rat pituitary gland, bovine chromaffin cells, rat gonadotrophs, smooth muscle cells, and dissociated neurons from the rat nucleus basalis, comparable values for κ_S between 50 and 150 have been found (see Neher, 1995). In contrast, κ_S was estimated to be >20 times larger in cerebellar Purkinje cells

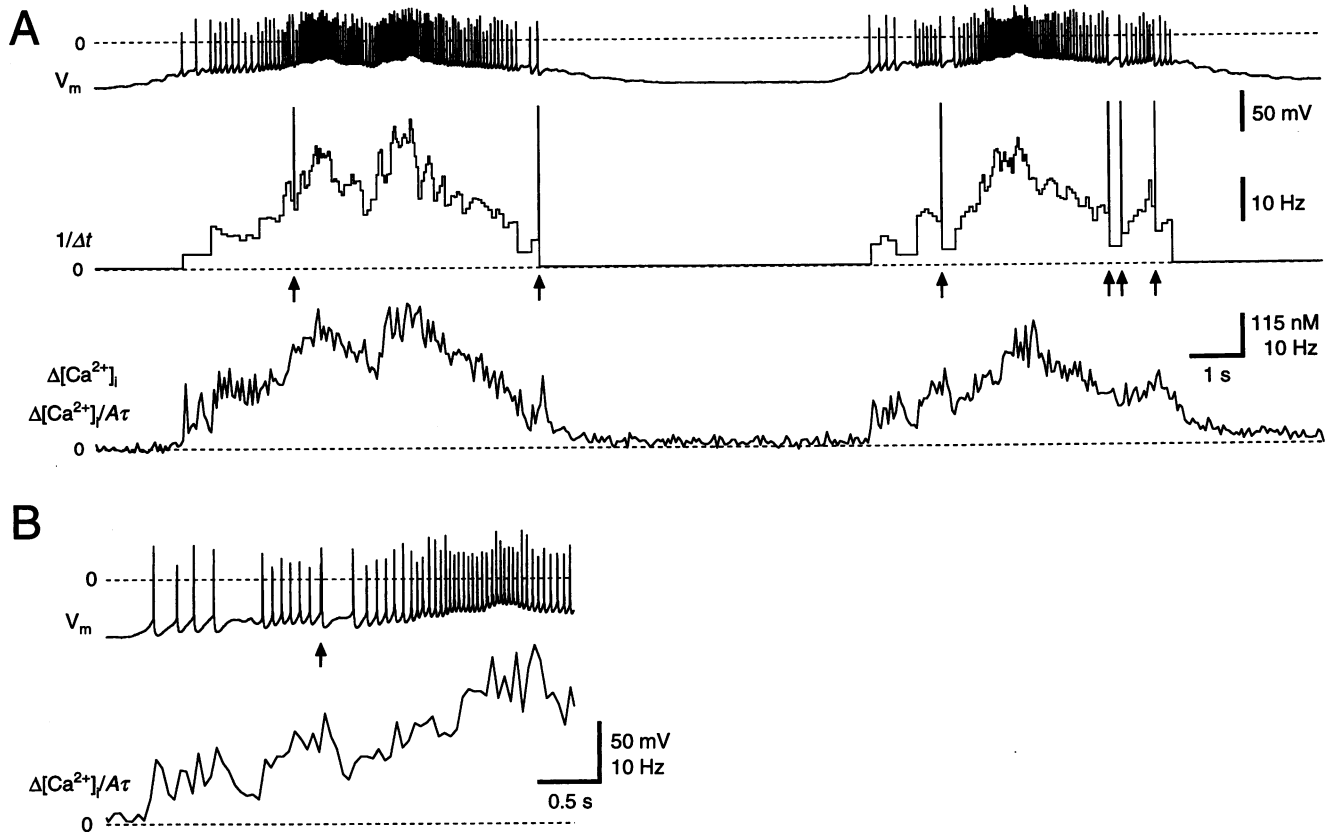

FIGURE 8 Encoding of action potential frequency by dendritic $[Ca^{2+}]_i$ levels. (*A*) (*Upper trace*) Membrane potential of a layer V pyramidal neuron (V_m) with trains of action potentials with variable frequency evoked by somatic current injection. Action potential peaks are truncated because of sampling at 1 kHz. (*Middle trace*) Time course of the instantaneous action potential frequency ($1/\Delta t$). Arrows indicate truncated peaks of the frequency curve, which were due to short bursts of two action potentials. (*Lower trace*) Simultaneously measured change of $[Ca^{2+}]_i$ in the proximal dendrite ($\Delta[Ca^{2+}]_i$, 20 Hz time resolution, 20 μM Fura-2). In addition to the scale in units of nM, a scale in units of Hz is shown, which was obtained by dividing $\Delta[Ca^{2+}]_i$ by $A\tau$ to convert it to "frequency." $A\tau$ was determined from amplitude and decay time constant of exponential curves fitted to $[Ca^{2+}]_i$ transients evoked by single action potentials, which were measured at 100 Hz acquisition rate before and after the bursts of action potentials. For these long measurements, B_{380}, B_{356}, and F_{356} were interpolated exponentially with a time constant determined from the decrease of fluorescence without stimulation. (*B*) Action potential pattern (V_m) and converted $[Ca^{2+}]_i$ signal ($\Delta[Ca^{2+}]_i/A\tau$) at the beginning of the second stimulation period on expanded time scale. The arrow indicates a short burst of two action potentials.

(Llano et al., 1994). This difference may reflect differences in the concentration and the species of cytoplasmic Ca^{2+} binding proteins. For example, studies with antibodies have shown that Ca^{2+} buffering proteins such as parvalbumin, calbindin-D28k, or calretinin are not present in most pyramidal neurons of the neocortex, whereas several types of GABAergic cells, including interneurons and cerebellar Purkinje cells, contain parvalbumin and calbindin-D28k (Baimbridge et al., 1992).

Knowledge of κ_S is important for interpreting fluorescence signals from Ca^{2+} indicators (Neher, 1995). It can be used to restrict the dye concentration required for a specific experiment. For example, if the error of $[Ca^{2+}]_i$ measurements in dendrites of pyramidal neurons should be <20%, the exogenously introduced Ca^{2+}-binding ratio should not exceed 20–40, corresponding to 10–20 μM Fura-2 (assuming $[Ca^{2+}]_{rest}$ = 50 nM). In addition, κ_S is an important parameter in modeling studies of dendritic Ca^{2+} signaling, which not only plays a role in Ca^{2+} buffering but also in Ca^{2+} diffusion (Jaffe et al., 1994; Wagner and Keizer, 1994; Zador and Koch, 1994).

Because the effect of Fura-2 on the size and time course of $[Ca^{2+}]_i$ transients was not markedly different with either continuous loading or loading for a short period (Figs. 3 and 5), we conclude that cytoplasmic Ca^{2+} buffers are relatively immobile and do not wash out during 15 min of whole-cell recording. We cannot exclude, however, washout of highly mobile Ca^{2+} buffers during the period of low access resistance in the short whole-cell experiments (30 s). Since the time constant of Fura-2 loading was 6 times longer (180 s), only about $(1 - e^{-1/6}) = 15\%$ of a buffer with similar molecular weight as Fura-2 ($M_{Fura\text{-}2}$ = 637 Da) would be lost during a period of 30 s, and even less (~6–8%) of a molecule with 10–20 kDa molecular weight, assuming a third-power relationship between molecular mass and diffusion time constant (Pusch and Neher, 1988). Thus, only Ca^{2+}-binding molecules with a molecular mass less than

Fura-2 could significantly wash out during a period of 30 s.

Dendritic Ca^{2+} accumulation during neuronal activity

In the somatosensory and visual cortical areas of the rat the "spontaneous" neuronal impulse rates increase from 0–10 Hz in the absence of stimulation to 20–50 Hz during sensory stimulation (Burne et al., 1984; Simons et al., 1992). Ca^{2+} accumulation in proximal dendrites during trains of action potentials is well described by linear superposition of the single $[Ca^{2+}]_i$ transients in the frequency range up to 30 Hz (Fig. 6). Thus, Ca^{2+}-induced Ca^{2+} release from internal stores is unlikely to contribute to this accumulation. In contrast, supralinear dendritic Ca^{2+} accumulation was observed during repetitive voltage pulses in cerebellar Purkinje cells and was attributed to Ca^{2+}-induced Ca^{2+} release (Llano et al., 1994). Ca^{2+} release within dendrites of pyramidal neurons, however, may be induced by other stimuli, such as synaptic activation of NMDA receptors (Alford et al., 1993).

Dendritic $[Ca^{2+}]_i$ rapidly reached a steady state during trains of action potentials with constant frequency. Therefore the time course of action potential frequency was well described by the Ca^{2+} signal during "physiological" patterns of neuronal activity (Fig. 8). In contrast, previous measurements showed a continuous slow rise of $[Ca^{2+}]_i$ during 0.5–1 s trains of action potentials, with $[Ca^{2+}]_i$ representing the number of action potentials that occurred rather than encoding their frequency (Jaffe et al., 1992, 1994; Miyakawa et al., 1992). This slow rise could be an effect of the higher Fura-2 concentrations used; the transients that were evoked by single action potentials decayed slowly in these experiments (time constant >500 ms), and as a result the time to reach steady state was prolonged as well (Eq. 7), and thus during 0.5–1 s a plateau was not yet reached.

After trains of action potentials we found a double-exponential decay of $[Ca^{2+}]_i$, as has also been reported by Regehr and Tank (1992) and Schiller et al. (1995). This finding disagrees with the linear superposition model of monoexponential transients described in Materials and Methods. Possible explanations are the decrease of Fura-2 Ca^{2+}-binding ratio during $[Ca^{2+}]_i$ buildup (Eq. 1), which causes a fastening of the decay at higher $[Ca^{2+}]_i$ levels (see also Tse et al., 1994), or the recruitment of Ca^{2+} buffers with slow kinetics during electrical activity. In addition, since the relative amplitudes of the two exponentials did not depend on the frequency of action potentials, there may have been a slow component in the transients evoked by single action potentials as well, which was not resolved because of baseline noise.

Action potential evoked dendritic Ca^{2+} signaling

$[Ca^{2+}]_i$ transients, evoked by single action potentials, have also been measured in distal and in oblique and basal dendrites (Spruston et al., 1995b; Schiller et al., 1995). Consistent with surface-to-volume considerations the transients were larger and faster in finer dendrites (Schiller et al., 1995). In addition, there is now evidence for the presence of voltage-activated Ca^{2+} channels in dendritic spines and for increases in $[Ca^{2+}]_i$ in spines evoked by single action potentials (Mills et al., 1994; Yuste and Denk, 1995; Segal, 1995). The undistorted "physiological" transients in fine dendrites and spines are likely to last <70 ms, but one cannot exclude spatial inhomogenities of Ca^{2+}-binding ratio and Ca^{2+} channel density. At least, measured $[Ca^{2+}]_i$ profiles in dendritic trees are consistent with a uniform Ca^{2+} channel distribution with the pattern of Ca^{2+} entry being determined by the spread of action potentials (Jaffe et al., 1992, 1994). This spread is activity-dependent in dendrites of hippocampal CA1 neurons (Jaffe et al., 1992). The first action potential in a train propagates into distal dendrites, whereas the following action potentials can fail to propagate, probably at dendritic branch points (Spruston et al., 1995b).

Thus, there exist two distinct retrograde Ca^{2+} signals in dendrites of pyramidal neurons: a widespread short transient increase of $[Ca^{2+}]_i$ after a single action potential, and a frequency-dependent buildup of $[Ca^{2+}]_i$ during trains of action potentials, which can be restricted to different parts of the dendritic tree. The first type of signal could serve to set conditions for the detection of coincident synaptic input. For example, Ca^{2+} that entered during an action potential could occupy binding sites of a cooperative Ca^{2+}-binding molecule near a postsynaptic density, and an additional highly localized Ca^{2+} inflow, e.g., through Ca^{2+}-permeable NMDA receptor channels, could lead to Ca^{2+} binding to additional sites. Yuste and Denk (1995) showed a supralinear buildup of $[Ca^{2+}]_i$ in spines after coincident synaptic activation and action potential invasion. Therefore, Ca^{2+} release from internal stores may be involved as well (Alford et al., 1993). The frequency-dependent dendritic Ca^{2+} changes during electrical activity may affect target molecules such as kinases and phosphatases, membrane conductances, and proteins affecting gene expression (Clapham, 1995; Lev et al., 1995; Kennedy, 1989; Gallin and Greenberg, 1995), and thus modulate cellular and dendritic function in an activity-dependent way.

We thank Dr. E. Neher for helpful discussions, Drs. J. G. G. Borst and G. J. Stuart for critically reading the manuscript, and M. Kaiser for expert technical assistance.

REFERENCES

Alford, S., B. G. Frenguelli, J. G. Schofield, and G. L. Collingridge. 1993. Characterization of Ca^{2+} signals induced in hippocampal CA1 neurons by the synaptic activation of NMDA receptors. *J. Physiol.* 469:693–716.

Baimbridge, K. G., M. R. Celio, and J. H. Rogers. 1992. Calcium-binding proteins in the nervous system. *Trends Neurosci.* 15:303–308.

Bekkers, J. M., and C. F. Stevens. 1989. NMDA and non-NMDA receptors are co-localized at individual excitatory synapses in cultured rat hippocampus. *Nature.* 341:230–233.

Bliss, T. V. P., and G. L. Collingridge. 1993. A synaptic model of memory: long-term potentiation in the hippocampus. *Nature.* 361:31–39.

Blumenfeld, H., L. Zablow, and B. Sabatini. 1992. Evaluation of cellular mechanisms for modulation of calcium transients using a mathematical model of fura-2 Ca^{2+} imaging in *Aplysia* sensory neurons. *Biophys. J.* 63:1146–1164.

Burne, R. A., J. G. Parnavelas, and C.-S. Lin. 1984. Response properties of neurons in the visual cortex of the rat. *Exp. Brain Res.* 53:374–383.

Carafoli, E., and M. Chiesi. 1992. Calcium pumps in the plasma and intracellular membranes. *Curr. Top. Cell. Regul.* 32:209–241.

Christie, B. R., L. S. Eliot, K.-I. Ito, H. Miyakawa, and D. Johnston. 1995. Different Ca^{2+} channels in soma and dendrites of hippocampal pyramidal neurons mediate spike-induced Ca^{2+} influx. *J. Neurophysiol.* 73: 2553–2557.

Clapham, D. E. 1995. Calcium signaling. *Cell.* 80:259–268.

Eilers, J., R. Schneggenburger, and A. Konnerth. 1995. Patch clamp and calcium imaging in brain slices. *In* Single-channel recording, 2nd ed. B. Sakmann and E. Neher, editors. Plenum Press, New York. 213–229.

Gallin, W. J., and M. E. Greenberg. 1995. Calcium regulation of gene expression in neurons: the mode of entry matters. *Curr. Opin. Neurobiol.* 5:367–374.

Groden, D. L., Z. Guan, and B. T. Stokes. 1991. Determination of Fura-2 dissociation constants following adjustment of the apparent Ca-EGTA association constant for temperature and ionic strength. *Cell Calcium.* 12:279–287.

Grynkiewicz, G., M. Poenie, and R. Y. Tsien. 1985. A new generation of Ca^{2+} indicators with greatly improved fluorescence properties. *J. Biol. Chem.* 260:3440–3450.

Jaffe, D. B., D. Johnston, N. Lasser-Ross, J. E. Lisman, H. Miyakawa, and W. N. Ross. 1992. The spread of Na^{+} spikes determines the pattern of dendritic Ca^{2+} entry into hippocampal neurons. *Nature.* 357:244–246.

Jaffe, D. B., W. N. Ross, J. E. Lisman, N. Lasser-Ross, H. Miyakawa, and D. Johnston. 1994. A model for dendritic Ca^{2+} accumulation in hippocampal pyramidal neurons based on fluorescence imaging measurements. *J. Neurophysiol.* 71:1065–1077.

Kennedy, M. B. 1989. Regulation of neuronal function by calcium. *Trends Neurosci.* 12:417–420.

Lasser-Ross, N., H. Miyakawa, V. Lev-Ram, S. R. Young, and W. N. Ross. 1991. High time resolution fluorescence imaging with a CCD camera. *J. Neurosci. Methods.* 36:253–261.

Lev, S., H. Moreno, R. Martinez, P. Canoll, E. Peles, J. M. Musacchio, G. D. Plowman, B. Rudy, and J. Schlesinger. 1995. Protein tyrosine kinase PYK2 involved in Ca^{2+}-induced regulation of ion channel and MAP kinase functions. *Nature.* 376:737–745.

Llano, I., R. DiPolo, and A. Marty. 1994. Calcium-induced calcium release in cerebellar Purkinje cells. *Neuron.* 12:663–673.

Magee, J. C., and D. Johnston. 1995. Characterization of single voltage-gated Na^{+} and Ca^{2+}-channels in apical dendrites of rat CA1 pyramidal neurons. *J. Physiol.* 487:67–90.

Markram, H., P. J. Helm, and B. Sakmann. 1995. Dendritic calcium transients evoked by single back-propagating action potentials in rat neocortical pyramidal neurons. *J. Physiol.* 485:1–20.

McCobb, D. P., and K. G. Beam. 1991. Action potential waveform voltage-clamp commands reveal striking differences in calcium entry via low and high voltage-activated calcium channels. *Neuron.* 7:119–127.

Mills, L. R., C. E. Niesen, A. P. So, P. L. Carlen, I. Spigelman, and O. T. Jones. 1994. N-type Ca^{2+} channels are located on somata, dendrites, and a subpopulation of dendritic spines on live hippocampal pyramidal neurons. *J. Neurosci.* 14:6815–6824.

Miyakawa, H., W. N. Ross, D. Jaffe, J. C. Callaway, N. Lasser-Ross, J. E. Lisman, and D. Johnston. 1992. Synaptically activated increases in Ca^{2+} concentration in hippocampal CA1 pyramidal cells are primarily due to voltage-gated Ca^{2+} channels. *Neuron.* 9:1163–1173.

Neher, E. 1995. The use of fura-2 for estimating Ca buffers and Ca fluxes. *Neuropharmacology.* 34:1423–1442.

Neher, E., and G. J. Augustine. 1992. Calcium gradients and buffers in bovine chromaffin cells. *J. Physiol.* 450:273–301.

Nowycky, M. C., and M. J. Pinter. 1993. Time courses of calcium and calcium-bound buffers following calcium influx in a model cell. *Biophys. J.* 64:77–91.

Pusch, M., and E. Neher. 1988. Rates of diffusional exchange between small cells and a measuring patch pipette. *Pflügers Arch.* 411:204–211.

Regehr, W. G., K. R. Delaney, and D. W. Tank. 1994. The role of presynaptic calcium in short-term enhancement at the mossy fibre synapse. *J. Neurosci.* 14:523–537.

Regehr, W. D., and D. W. Tank. 1992. Calcium concentration dynamics produced by synaptic activation of CA1 hippocampal pyramidal cells. *J. Neurosci.* 12:4202–4223.

Regehr, W. D., and D. W. Tank. 1994. Dendritic calcium dynamics. *Curr. Opin. Neurobiol.* 4:373–382.

Rexhausen, U. 1992. Bestimmung der Diffusionseigenschaften von Fluoreszenzfarbstoffen in verzweigten Nervenzellen unter Verwendung eines rechnergesteuerten Bildverarbeitungssystems. Diploma thesis. University of Göttingen.

Sala, F., and A. Hernández-Cruz. 1990. Calcium diffusion modeling in a spherical neuron. *Biophys. J.* 57:313–324.

Schiller, J., F. Helmchen, and B. Sakmann. 1995. Spatial profile of dendritic calcium transients evoked by action potentials in rat neocortical pyramidal neurones. *J. Physiol.* 487:583–600.

Segal, M. 1995. Fast imaging of $[Ca]_i$ reveals presence of voltage-gated calcium channels in dendritic spines of cultured hippocampal neurons. *J. Neurophysiol.* 74:484–488.

Simons, D. J., G. E. Carvell, A. E. Hershey, and D. P. Bryant. 1992. Responses of barrel cortex neurons in awake rats and effects of urethane anesthesia. *Exp. Brain Res.* 91:259–272.

Spruston, N., P. Jonas, and B. Sakmann. 1995a. Dendritic glutamate receptor channels in rat hippocampal CA3 and CA1 pyramidal neurons. *J. Physiol.* 482:325–352.

Spruston, N., Y. Schiller, G. Stuart, and B. Sakmann. 1995b. Activity-dependent action potential invasion and calcium influx into hippocampal CA1 dendrites. *Science.* 268:297–300.

Stuart, G. J., H.-U. Dodt, and B. Sakmann. 1993. Patch-clamp recordings from the soma and dendrites of neurons in brain slices using infrared video microscopy. *Pflügers Arch.* 423:511–518.

Stuart, G. J., and B. Sakmann. 1994. Active propagation of somatic action potentials into neocortical pyramidal cell dendrites. *Nature.* 367:69–72.

Stuart, G. J., and N. Spruston. 1995. Probing dendritic function with patch pipettes. *Curr. Opin. Neurobiol.* 5:389–394.

Timmerman, M. P., and C. C. Ashley. 1986. Fura-2 diffusion and its use as an indicator of transient free calcium changes in single striated muscle cells. *FEBS Lett.* 209:1–8.

Tse, A., W. Tse, and B. Hille. 1994. Calcium homeostasis in identified rat gonadotrophs. *J. Physiol.* 477:511–525.

Westenbroek, R. E., M. K. Ahlijanian, and W. A. Catterall. 1990. Clustering of L-type Ca^{2+} channels at the base of major dendrites in hippocampal pyramidal neurons. *Nature.* 347:281–284.

Wagner, J., and J. Keizer. 1994. Effects of rapid buffers on Ca^{2+} diffusion and Ca^{2+} oscillations. *Biophys. J.* 67:447–456.

Yuste, R., and W. Denk. 1995. Dendritic spines as basic functional units of neuronal integration. *Nature.* 375:682–684.

Zador, A., and C. Koch. 1994. Linearized models of calcium dynamics: Formal equivalence to the cable equation. *J. Neurosci.* 14:4705–4715.

Zhou, Z., and E. Neher. 1993. Mobile and immobile calcium buffers in bovine adrenal chromaffin cells. *J. Physiol.* 469:245–273.